Proceedings of Lunar and Planetary Science, Volume 22, pp. 127–136
Lunar and Planetary Institute, Houston, 1992

NMR Spectroscopy of Experimentally Shocked Quartz and Plagioclase Feldspar Powders

Randall T. Cygan

Geochemistry Division, Sandia National Laboratories, Albuquerque NM 87185

Mark B. Boslough

Structural Physics and Shock Chemistry Division, Sandia National Laboratories, Albuquerque NM 87185

R. James Kirkpatrick

Department of Geology, University of Illinois, Urbana IL 61801

Magic-angle spinning nuclear magnetic resonance (MAS NMR) spectroscopy is an extremely sensitive and reproducible probe of disorder in synthetic quartz powder samples that have been experimentally shock loaded to peak pressures up to 22 GPa. Careful curve fitting and deconvolution of ^{29}Si NMR spectra of shocked quartz leads to four primary observations: (1) the width of the resonance increases systematically with shock pressure, indicating a greater distribution of local silicon environments caused by shock-induced disorder; (2) a much broader peak component appears, indicating the presence of highly disordered material, which TEM observation indicates may be due to very high dislocation densities; (3) the disordered material appears to have a significantly shorter T_1 relaxation time than the crystalline material; and (4) there is no evidence for the presence of high-pressure silica phases (coesite or stishovite) in the shocked samples. The net effect of shock loading on the ^{29}Si NMR spectrum of quartz is an increase in peak width that strongly and consistently correlates with known shock pressure. Peak width is therefore a useful "shock barometer" for quartz in this pressure range for the experimental loading conditions. By contrast, ^{23}Na, ^{27}Al, and ^{29}Si MAS NMR spectra of shocked and unshocked An_{60} plagioclase feldspar powders do not change significantly with increasing shock pressure. There is no evidence for either amorphous or high-pressure phases in the plagioclase spectra for shock pressures up to 22 GPa.

INTRODUCTION

Identification of shocked minerals and determination of their degree of shock metamorphism has become an increasingly important problem in earth and planetary science as the relative importance of impact processes has been recognized. Diagnostic methods for examining shock features in minerals have traditionally relied on qualitative examination of microstructures by optical and electron microscopy. The object of much research has been to describe and characterize shock effects, thus providing criteria for recognizing and classifying various levels of shock metamorphism. Because shock features have been studied mainly with microscopic techniques, most of the descriptions have been of microstructural changes. These changes include twinning, recrystallization, glass formation, kink band formation, mosaic extinction, and formation of a number of types of planar and subplanar features called "planar deformation features," including microfault zones, fractures, glassy plates, and shock lamellae. Shock effects on mineral microstructures have been discussed extensively (for example, *Carter,* 1965; *French and Short,* 1968; *Kieffer,* 1971; *Stöffler,* 1972; *Roddy et al.,* 1977; *Grieve,* 1987; *Gratz,* 1984; *Gratz et al.,* 1988; *Alexopoulos et al.,* 1988; *Carter et al.,* 1989; *Nicolaysen and Reimold,* 1990).

An important use of these observations has been the identification of natural impacts on Earth. For example, recognition of shocked minerals at the Cretaceous-Tertiary boundary has been essential in linking the biological extinction that occurred at that time with an impact event (*Bobor et al.,* 1984; *French,* 1990). There has been some controversy in this interpretation, and some workers have suggested that mineral "shock features" may result from volcanic eruption processes (see *Carter et al.,* 1986). However, these concerns appear to have largely been laid to rest (*French,* 1990).

More quantitative methods including refractivity, density, X-ray diffraction (XRD), infrared absorption spectroscopy, X-ray photoelectron spectroscopy (XPS), and electron paramagnetic resonance (EPR) have also been used to investigate the physical state of shocked minerals and glasses (see *Stöffler,* 1984). Most of the data from these techniques show some degree of correlation with intensity of shock loading over some range of shock pressure in certain minerals, and have been used to identify shocked minerals and quantify their level of shock metamorphism.

We have previously shown that solid-state NMR is an extremely sensitive probe of disorder brought about by shock loading of quartz, and have suggested that it could be used as a "shock barometer" over a limited range of shock pressures and loading conditions (*Cygan et al.,* 1990). That work noted a good correlation between the width of the ^{29}Si resonance and known shock pressure. This correlation has a stronger dependence on shock pressures between 7.5 and 22 GPa than quantitative data determined by refractivity and XRD. That study was preliminary and rather empirical in nature, and the shock-induced structural changes responsible for the changes in the NMR spectra were not significantly explored.

We have now expanded on the earlier work by (1) repeating the experiments under the same conditions; (2) charac-

terizing the ^{29}Si MAS NMR spectra using better curve-fitting and deconvolution techniques; (3) examining the effect of postshock hydrofluoric acid etching and thermal annealing of quartz on the observed NMR spectra; (4) exploring the T_1 NMR relaxation of the shocked quartz; and (5) determining whether a more complex aluminosilicate mineral (An_{60} plagioclase feldspar) also exhibits a useful correlation between shock pressure and NMR spectral features. Our primary purpose is to determine the degree of reproducibility of the previous experimental results, to seek a physical basis for them, and to begin to determine whether they are unique to quartz. By understanding the source of the spectral changes, we expect to gain a stronger basis for using their correlation with shock pressure as a "shock barometer."

EXPERIMENTAL METHODS

The six shock recovery experiments using quartz powder samples were carried out in precisely the same manner as those for the study of *Cygan et al.* (1990). Well-characterized shock states were achieved by using the Sandia "Momma Bear" explosive loading fixtures, for which peak pressures and temperatures have been numerically determined by *Graham and Webb* (1984, 1986). Two sets of three experiments were performed, each to mean peak shock pressures of 7.5, 16.5, and 22 GPa. The only difference between the two sets were the initial packing densities of the powders, which lead to "low shock temperature" and "high shock temperature" conditions at the same shock pressures (Table 1). There are ranges of pressures and temperatures for each sample because the experimental shock loading is not uniform, and according to numerical simulations has a radial dependence. The samples for which the NMR spectra were obtained were taken from the bulk region where this dependence is weak and can be approximated by its mean value.

As with the previous study, the starting material was synthetic α-quartz sieved to a mean grain size of less than 38 μm (325 mesh). The only substantive difference in preparation procedure was that in the present study the quartz was annealed at 900°C for 20 hr to minimize the initial defect densities that had previously broadened the (101) X-ray diffraction peak.

One set of three shock-loading experiments was carried out on an An_{60} plagioclase feldspar (labradorite). The initial packing density led to relatively high shock temperatures (Table 1). The natural An_{60} plagioclase is from a basalt flow from Pueblo Park, New Mexico, and was pretreated by annealing at 900°C for 20 hr before shock loading.

The NMR experiment detects the radio frequency emission from active nuclei that have been excited to high-energy spin states while the sample is located in a very strong magnetic field. *Wilson* (1987) and *Kirkpatrick* (1988) discuss MAS NMR spectroscopy and its application to minerals. Our ^{29}Si MAS NMR spectra were obtained at a frequency of 71.5 MHz with an applied magnetic field of 8.45 T and the identical experimental conditions as those used by *Cygan et al.* (1990). The ^{23}Na and ^{27}Al MAS NMR spectra for the plagioclase samples were obtained at 130.3 MHz and 132.3 MHz respectively using a similar spectrometer and an applied magnetic field of 11.74 T. In all cases, the spectra were taken under magic-angle spinning (MAS) conditions to reduce the broadening associated with quadrupolar interactions. The spinning rate was approximately 3.5 kHz. Pulse Fourier transform methods were used in which signals are detected in the time domain and then transformed to the frequency domain.

The NMR chemical shifts are referenced to tetramethylsilane (TMS) (^{29}Si), 1 molar NaCl solution (^{23}Na), and 1 molar $AlCl_3$ solution (^{27}Al), with increased shielding for less positive or more negative values. All the MAS NMR spectra were obtained using a pulse recycle time of 30 s unless otherwise noted. The effects of varying recycle times on the ^{29}Si resonance of SiO_2 minerals are briefly discussed by *Yang et al.* (1986).

RESULTS AND DISCUSSION

Thermal Annealing of Quartz

Because we were concerned that the initial defect structure could have a significant effect on the NMR spectra and X-ray diffraction patterns, we explored the effect of thermal annealing of the quartz without shock loading. We heated the synthetic quartz to various temperatures for times of 1 hr and about 20 hr and measured the effects on the ^{29}Si resonance and the (101) X-ray diffraction peak (see Table 2). The widths

TABLE 1. Schedule of shock recovery experiments.

Shot	Fixture	Explosive	Initial Sample Compact Density (Mg/m^3)	Initial Sample Compact Density (%)	Peak Pressure (GPa)	Estimated Mean Bulk Temperature (°C)
Quartz						
8B906	Momma Bear	Baratol	1.60	60	5-10	150-175
5B906	Momma Bear	Comp B	1.60	60	13-20	325-475
2B906	Momma Bear-A	Comp B	1.60	60	18-26	325-575
9B906	Momma Bear	Baratol	1.36	51	5-10	300-325
6B906	Momma Bear	Comp B	1.36	51	13-20	475-600
3B906	Momma Bear-A	Comp B	1.36	51	18-26	450-700
An_{60} Plagioclase Feldspar						
7B906	Momma Bear	Baratol	1.30	48	5-10	325-350
4B906	Momma Bear	Comp B	1.30	48	13-20	500-625
1B906	Momma Bear-A	Comp B	1.30	48	18-26	500-725

TABLE 2. Narrowing of measured peaks for annealed quartz powders.

Anneal Conditions		Peak Width Relative to Initial (%)	
Temperature (°C)	Time (hr)	X-ray (101)	NMR (-107 ppm)
700	1	93	93
700	16	90	91
900	1	79	85
900	17	81	92
900	20	81	89
1100	1	86	89
1100	17	80	90

of both NMR and XRD peaks decrease with heat treatment, but the decrease in NMR peak width is insignificant relative to the broadening caused by the shock loading. The change in width of the XRD peak, however, is of the same order as the shock-induced broadening (*Cygan et al.*, 1990). The peak widths were determined by fitting a split Pearson VII function to the observed data (see appendix). The peak width values reported in Table 2 have a relative error (one estimated standard deviation) of approximately 5% to 12% based upon the curve-fitting procedure. Because of these results, we used annealed quartz as our starting material for the shock studies, but there is no effect on the comparison of the present NMR results with those of *Cygan et al.* (1990).

Shock-Induced Broadening of Quartz ^{29}Si NMR Resonance

The ^{29}Si MAS NMR spectra for the six shocked quartz samples of the present study show systematic increases in peak width with increasing shock pressure for both the low and high shock temperature experiments (Figs. 1 and 2). To better compare NMR peak widths we now make use of a systematic approach to spectral fitting that eliminates measurement error and bias. In this method the spectra are fit by a split Pearson VII function. This function has six adjustable parameters, from which one that represents the full width at half-maximum height (peak width) can be defined. This function was used because it is asymmetrical (like the observed NMR data) and because it represents a combination of Lorentzian and Gaussian functions. The appendix contains a description of the split Pearson VII function and provides details of the fitting parameters.

Similar broadening of the ^{29}Si resonance in shocked quartz was observed by *Cygan et al.* (1990), who attributed it to either extensive disordering and residual strain or formation of an amorphous phase, or some combination of these contributions. They concluded that the broadening correlates to an increase in the range of mean Si-O-Si bond angles per tetrahedron in the shocked samples. The key finding of that work, however, was the strong correlation between peak breadth and shock pressure.

The ^{29}Si MAS NMR peaks of the annealed unshocked and shocked quartz samples are well fit by the split Pearson VII function (Fig. 3). The peak widths of the shocked samples normalized to that of the starting material increase systematically with increasing shock pressure for both the high and low

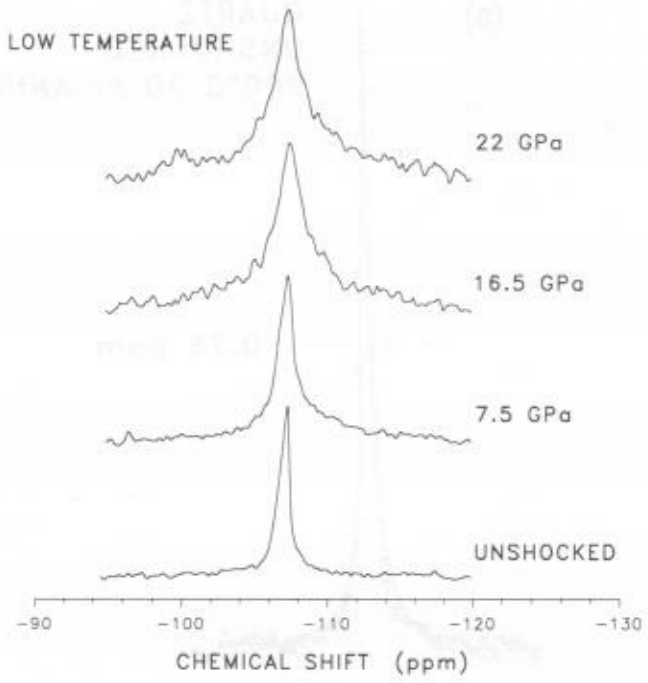

Fig. 1. Silicon-29 MAS NMR spectra for unshocked starting material and shocked quartz powders obtained for the low shock temperature set of recovery experiments.

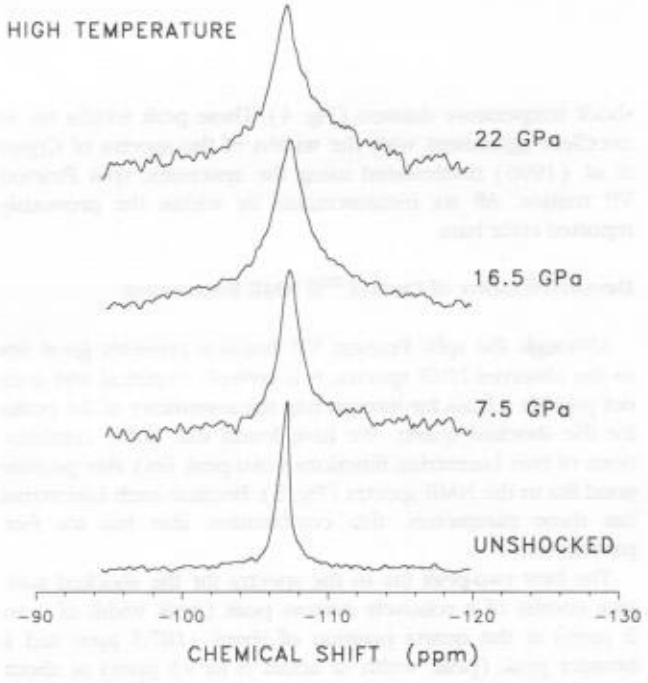

Fig. 2. Silicon-29 MAS NMR spectra for unshocked starting material and shocked quartz powders obtained for the high shock temperature set of recovery experiments.

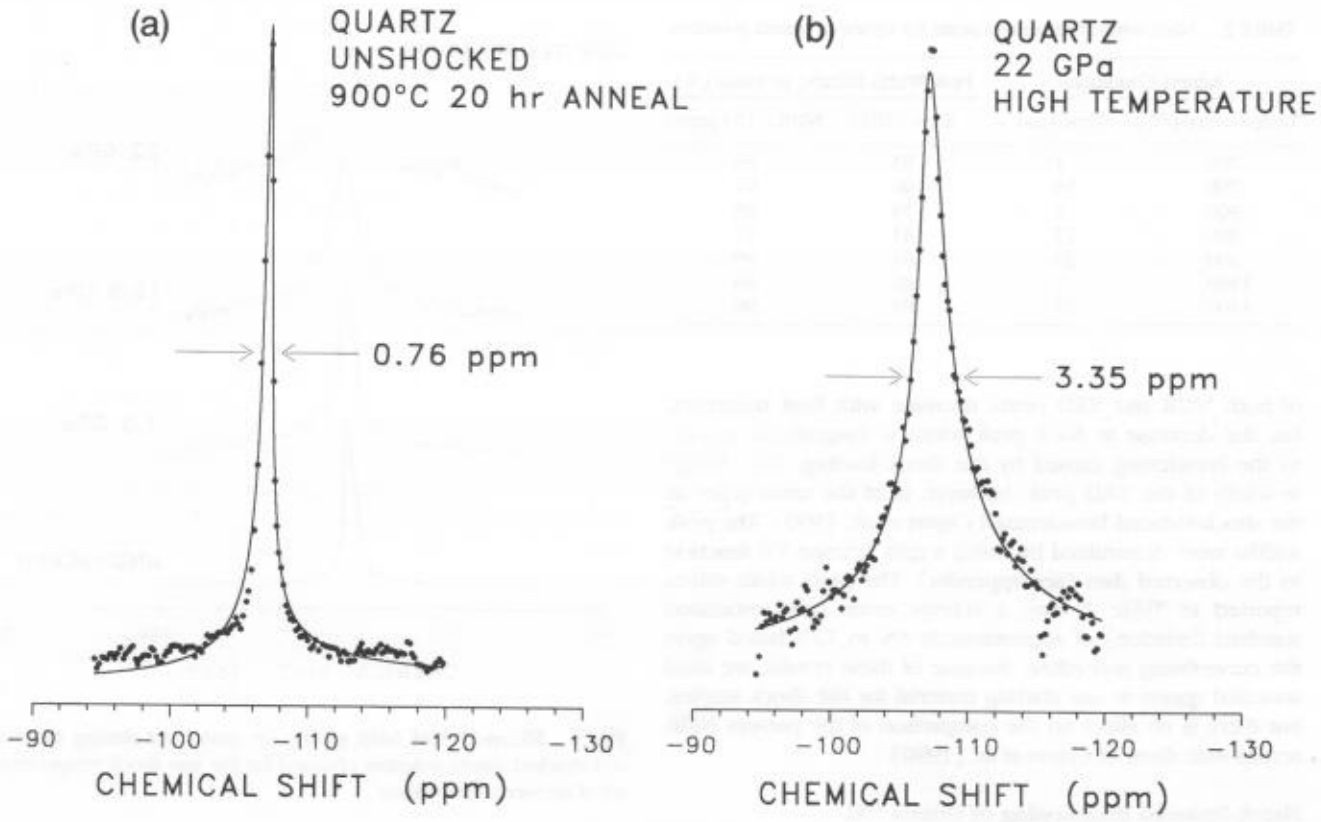

Fig. 3. Comparison of ^{29}Si MAS NMR spectra with split Pearson VII curve fits: **(a)** annealed (900°C for 20 hr) quartz starting material and **(b)** 22-GPa high shock temperature quartz sample.

shock temperature datasets (Fig. 4). These peak widths are in excellent agreement with the widths of the spectra of *Cygan et al.* (1990) recalculated using the systematic split Pearson VII routine. All six measurements lie within the previously reported error bars.

Deconvolutions of Quartz ^{29}Si NMR Resonance

Although the split Pearson VII function provides good fits to the observed NMR spectra, it is entirely empirical and does not provide a basis for interpreting the asymmetry of the peaks for the shocked quartz. We have found that linear combinations of two Lorentzian functions (two-peak fits) also provide good fits to the NMR spectra (Fig. 5). Because each Lorentzian has three parameters, this combination also has six free parameters.

The best two-peak fits to the spectra for the shocked samples consist of a relatively narrow peak (peak width of 1 to 2 ppm) at the quartz position of about -107.3 ppm and a broader peak (peak width of about 8 to 13 ppm) at about -108 ppm. The narrow peak can be taken to represent silicon on sites that are not greatly distorted from the original quartz structure, and the broad peak to represent silicon on more

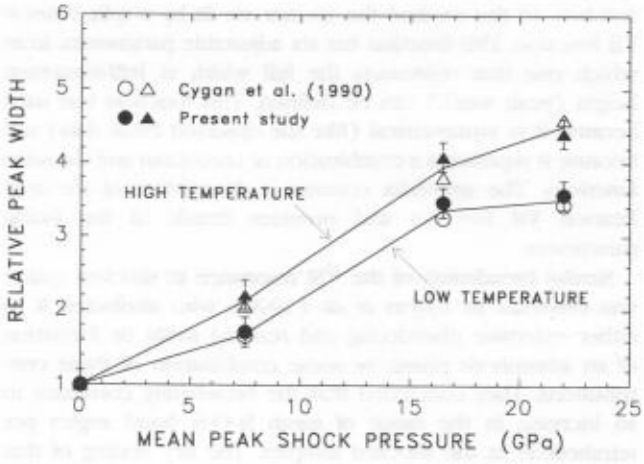

Fig. 4. Silicon-29 MAS NMR peak widths of the shocked quartz powders normalized to that of the unshocked starting material vs. the mean peak shock pressure. Open symbols represent data from the initial study of *Cygan et al.* (1990) and the filled symbols are the data from the present study. For clarity, error bars are presented only for the data from the present study.

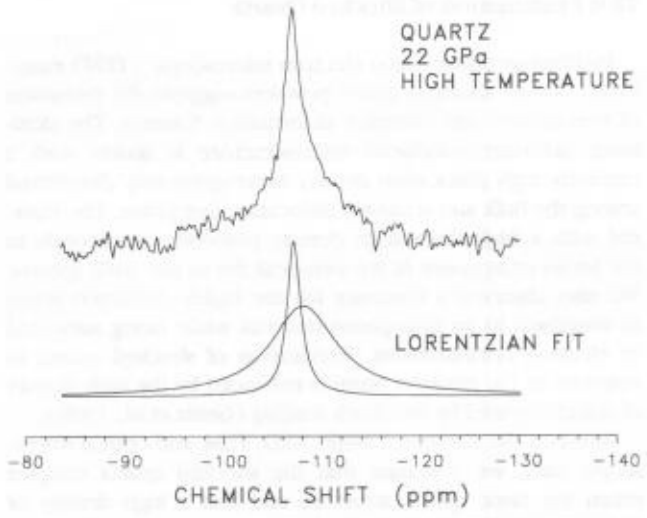

Fig. 5. Silicon-29 MAS NMR spectrum for the 22-GPa high shock temperature quartz sample and the deconvolution of the spectrum with two Lorentzian peaks.

distorted sites. The two-peak fit, however, is only a useful formalism, and the observation that the split Pearson VII function fits the peaks as well probably indicates that there is a continuum of silicon environments in the shocked samples. The chemical shift of about -108 ppm for the broad peak indicates an increase of average mean Si-O-Si bond angle per tetrahedron from about 144° for unshocked quartz to about 146° for the sites represented by the peak. *Pettifer et al.* (1988) provides a discussion of this correlation of bond angle with NMR chemical shift for silica materials.

The broad peak is significantly different from that for typical amorphous silica. Silica glasses, for instance, have peak maxima at about -111 to -112 ppm and peak widths of 10 ppm or more (*Dupree and Pettifer,* 1984; *Oestrike et al.,* 1987; *Pettifer et al.,* 1988). Thus, the sites represented by the broad peak in our two-peak fits have a smaller average mean Si-O-Si bond angle per tetrahedron and a narrower range of mean Si-O-Si bond angles than most amorphous silica. This result is consistent with the lack of evidence for an amorphous phase in X-ray diffraction and optical microscopic observations.

There is no evidence of additional crystalline silica phases in any of the measured ^{29}Si NMR spectra for the shocked quartz powders. In particular, there are no peaks for coesite (-108.1 ppm and -113.9 ppm) or for the sixfold silicon in stishovite (-191.1 ppm) (see *Smith and Blackwell,* 1983; *Yang et al.,* 1986).

Effects of Postshock Treatment on ^{29}Si NMR Resonance

Further evidence for the association of the broad spectral component with highly distorted sites comes from the reduction in ^{29}Si NMR peak width of shocked quartz after partial dissolution in hydrofluoric acid (Fig. 6). A split Pearson VII curve fitted to the spectrum of the 22-GPa high shock temperature sample etched for 30 s in a 1:1 diluted hydrofluoric acid solution indicates a 32% reduction in peak width after reaction. The two-peak fit indicates that the narrowing can be attributed primarily to a decrease in the intensity of the broad peak (Fig. 6). Similar effects are observed for the 16-GPa high shock temperature sample. These results are consistent with the expected selective dissolution of highly deformed material.

Similar changes in the ^{29}Si resonance are caused by postshock thermal annealing of the powders. Annealing of the 22-GPa and 16.5-GPa high shock temperature powders at 900°C for 20 hr causes the split Pearson VII peak widths to decrease by 8% and 18% respectively. Two-peak fits of the spectra indicate decreases in the breadths of both resonance components. The relative intensity of the broad peak is also reduced by 24% and 14% for the 22-GPa and 16.5-GPa high shock temperature samples respectively. These observations are consistent with thermal annealing of defects in the deformed material.

Relaxation Effects

The relative intensities of the broad peaks in the two-peak fits are greater than those of the narrow peaks in the MAS NMR spectra obtained with a pulse recycle of 30 s. For fully relaxed resonances, these areas should be proportional to the relative atomic abundances of the corresponding sites. If one type of site relaxes much faster than the other and if one or both of the resonances are not fully relaxed, the relative intensity of the fast-relaxing site would be enhanced. To examine the effect of recycle time on the shapes and relative areas of the fitted peaks, ^{29}Si MAS NMR spectra were also obtained for the 22-GPa high shock temperature sample using recycle times of 5 s and 300 s.

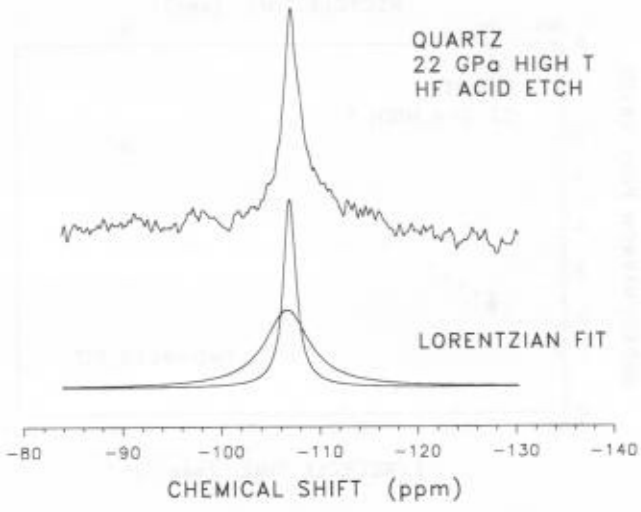

Fig. 6. Silicon-29 MAS NMR spectrum for the 22-GPa high shock temperature quartz sample after treatment with hydrofluoric acid and the deconvolution of the spectrum with two Lorentzian peaks.

For our samples the relative intensity (area) of the broad peak in the two-peak fit decreases with increasing recycle time (Fig. 7), indicating that the silicons on the site represented by this broad peak have a shorter T_1 average relaxation time than the silicons represented by the narrow peak. This difference can be explained by postulating a higher concentration of paramagnetic centers associated with defects near the more distorted sites. Such paramagnetic centers could be due to unpaired electrons associated with unsatisfied bonds or dislocations or point defects.

Recent evidence indicates that the time dependence of magnetization recovery for isotopically dilute spins such as ^{29}Si follows a power law rather than exponential decay, and that for spins that are relaxed by interaction with paramagnetic impurities, the exponent of the power-law decay is related to the fractal dimension of the associated phase (*Devreux et al.*, 1990). To explore this possibility, we have obtained preliminary data indicating that both the narrow and broad components indeed have power-law dependences, with saturation times of the order of 10^3 and 10^5 s for the broad and narrow components respectively (R. Assink, unpublished data, 1991). The observed power-law exponents are consistent with fractal dimensions of about 3 for the narrow component and of 1.5 to 2 for the broad component.

Using the power-law functions to fit the relaxation behavior indicates that the actual relative intensity of the broad peak may be in the range of 0.3% to 1.0%, rather than the 50% to 80% estimated from the fit to the short recycle-time spectra. Thus, the opportunity to characterize the extensive distorted silicon environments represented by the broad component is a fortuitous result of the T_1 relaxation behavior of these samples.

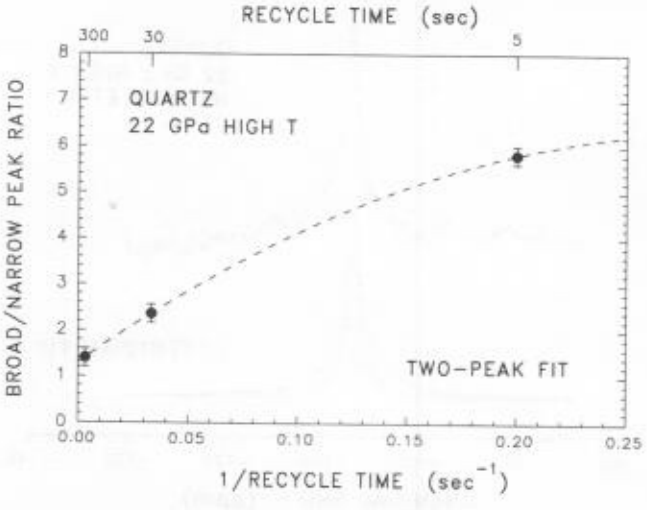

Fig. 7. Ratio of the intensities of the broad and narrow components of the two-peak fits vs. reciprocal recycle time for the ^{29}Si MAS NMR spectra of the 22-GPa high shock temperature quartz sample.

TEM Examination of Shocked Quartz

Preliminary transmission electron microscopic (TEM) examination of the shocked quartz powders suggests the formation of nonuniform and complex deformation features. The dominant deformation-induced microstructure is quartz with a relatively high dislocation density heterogeneously distributed among the bulk and relatively dislocation-free phase. The material with a high dislocation density probably corresponds to the broad component of the two-peak fits to the NMR spectra. We also observed a tendency for the highly deformed phase to transform to an amorphous material while being subjected to electron bombardment. Vitrification of shocked quartz in response to the electron beam is enhanced by the high density of defects created by the shock loading (*Gratz et al.*, 1988).

Based on the combined NMR, XRD, TEM, and optical microscopic data, we conclude that the shocked quartz samples retain the basic quartz structure and that a high density of dislocations causes the wide observed range of local silicon environments and the slight increase in the mean Si-O-Si bond angle.

Quartz NMR Shock Barometer

The results presented above indicate that the shock barometer suggested by *Cygan et al.* (1990) can be a useful empirical tool, albeit with a number of important qualifications, and that the peak width as determined by the split Pearson VII function is more reproducible than relative peak intensities in the two-peak fits (see Figs. 4 and 8). The correlation of relative peak intensities with shock pressure is still strong, but there is significant scatter and the reproducibility is not as good as for the split Pearson VII peak widths. We believe that the larger scatter in the two-peak fits is a result of the difficulty of doing the fits and that the split Pearson VII peak widths provide a better correlation with peak shock pressure because they are less subject to statistical fitting errors.

The interpretations discussed above also provide a fundamental basis for understanding the origin of the correlation. Increasing shock loading causes increased structural distortions and an increased amount of deformed material.

It must be emphasized that this shock barometer has only been calibrated for specific loading conditions. There has always been a tendency to relate the results of shock recovery experiments only to peak pressure. Such an interpretation neglects other aspects of the shock process that may have as much or more influence on the result (*Kieffer*, 1971; *Stöffler*, 1972). In practice the shock wave is a short stress pulse, with the shock front followed by a faster rarefaction wave that decreases the peak pressure and increases the duration of the pulse as the wave propagates. The pulse duration in laboratory experiments is typically about a microsecond, whereas large natural impacts can have pressure durations of up to a second. Comparison between laboratory shocked and naturally shocked samples of effects that require more than a microsecond to develop are clearly questionable. A clear difference is the formation of coesite, which is present at meteorite craters but is not produced in laboratory recovery experiments with short pressure durations (*DeCarli and Milton*, 1965; this study) or

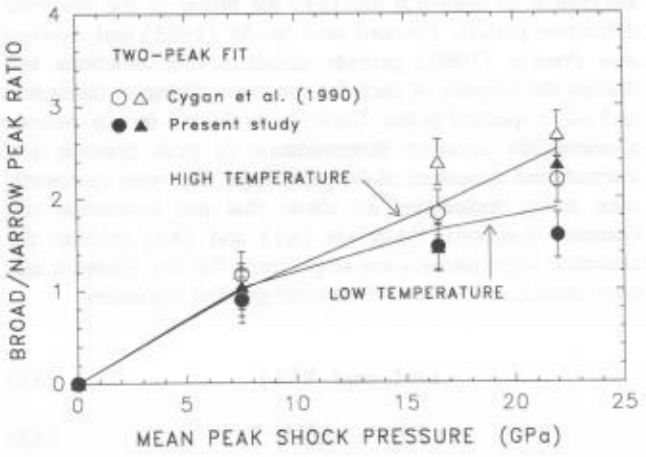

Fig. 8. Ratio of the intensities of the broad and narrow components of the two-peak fits to the ^{29}Si MAS NMR spectra vs. mean peak shock pressure. Open symbols are data from the initial study of *Cygan et al.* (1990) and filled symbols are the data of the present study.

is only produced in minute quantities (*Deribas et al.*, 1965). In future research we intend to carry out a systematic study of naturally shocked quartz to determine under what circumstances, if any, the experimental NMR shock barometer can be applied.

Another complication in applying the NMR shock barometer to natural samples is that the approach to peak pressure is in practice not an instantaneous event. For a single shock wave the true rise time depends on such material properties as yield strength, the existence of phase transitions, viscosity, and thermal transport. The geometry of our laboratory experiments leads to shock reverberations, whereby the sample is brought to the peak pressure in steps. Shock reverberations also occur in nature, because most rocks are polycrystalline and have some porosity. Stress waves can reflect off grain boundaries and free surfaces, giving rise to wide variations in local conditions. The high strain rates associated with rapid pressure release and tensile pulses following the shock wave can also generate effects that might be attributed to the shock wave.

Finally the postshock temperature history of the material can have an effect on the observed properties. This temperature depends on the initial porosity and loading path, as well as on the peak shock pressure. The cooling time depends on details of the experimental geometry for laboratory shocked samples and on depth of burial and thermal transport properties for a natural event. Of all these potentially complicating factors, the only ones we have significantly addressed have to do with temperature. The relative peak widths depend on shock temperature (or initial packing density) as well as on shock pressure (Fig. 4). However, the initial densities of quartz powders used in this study are quite low compared to those likely to be naturally shocked, and a more complete study would require denser initial states. Because postshock annealing of our samples at 900°C for 20 hr has some effect on the resulting NMR spectra (10% to 20% peak width decrease), we express some concern in applying the shock barometer to material of unknown thermal history.

Another important problem is that the dependence of relative peak intensity on shock pressure (Fig. 8) is only valid for NMR experiments with recycle times of 30 s and for samples with similar T_1 relaxation time. Figure 7 illustrates the strong dependence of this parameter on recycle time for our material. If relaxation to paramagnetic defects controls the T_1 values, relative intensities of the fitted peaks and the overall peak width must also depend on the concentration of paramagnetic sites in the quartz.

Perhaps the most important result of this study is not a method of determining the shock pressure for an unknown sample, but a method of *identification* of shocked quartz. Even in our most highly shocked quartz sample, we found very few grains with the diagnostic optical features normally used to identify shocked quartz, and no high-pressure phases are detected by XRD or MAS NMR. However, the ^{29}Si NMR resonances are significantly broadened, with the broadening strongly correlated with shock pressure. We suggest that this broadening can be effectively used as a convenient, new diagnostic technique for identifying naturally shocked quartz.

NMR Spectra of Shocked An_{60} Plagioclase

The ^{23}Na, ^{27}Al, and ^{29}Si MAS NMR spectra of the shocked An_{60} plagioclase feldspar are not significantly different from those of the unshocked sample. This sample probably has the incommensurate, modulated structure characteristic of such feldspar (see *Ribbe*, 1983). The ^{29}Si MAS NMR spectra of intermediate plagioclase feldspars are complex due to the large number of silicon sites and the incommensurate structure (see *Kirkpatrick et al.*, 1986, 1987, and *Kirkpatrick*, 1988 for a summary of the NMR results for plagioclase feldspar). The ^{29}Si MAS NMR spectra of the unshocked and shocked samples (Fig. 9) consist of multiple overlapping resonance in the range

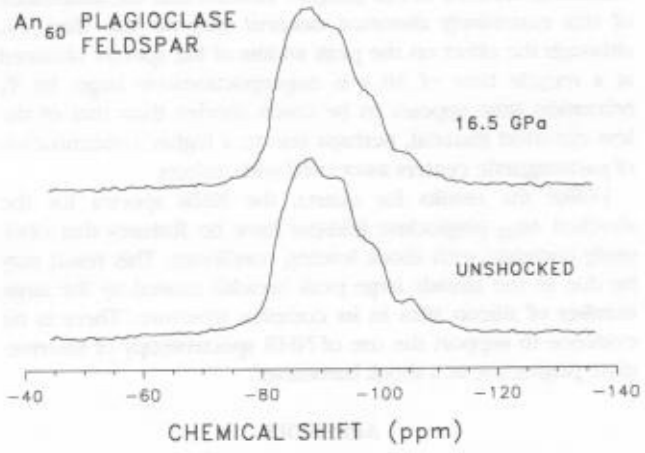

Fig. 9. Silicon-29 MAS NMR spectra of the annealed (900°C for 20 hr) An_{60} plagioclase starting material and the 16.5-GPa shocked plagioclase feldspar.

of -80 to -111 ppm and are similar to those previously observed (*Kirkpatrick et al.*, 1987). Deconvolutions of these spectra require either six or seven peaks that represent the wide distribution of silicon environments in the incommensurate structure, and there is no significant correlation of any fitted parameter with shock pressure.

The ^{27}Al peaks have maxima at about +54 ppm and widths of 28 ppm. The ^{23}Na peaks have maxima at about -18 ppm and widths of about 18 ppm. These NMR spectra are also similar to previously published spectra (*Kirkpatrick et al.*, 1985).

CONCLUSIONS

Silicon-29 MAS NMR spectroscopy of quartz powders is exceptionally sensitive to disorder produced by shock loading to pressures between 7.5 and 22 GPa. The level of disorder increases with shock pressure in such a way as to increasingly broaden the ^{29}Si resonance. The chemical shifts and widths of the peaks for the shocked quartz, in combination with the lack of optical and XRD evidence for an amorphous phase, suggest that the observed peak broadening is due to changes in Si-O-Si bond angles caused by large dislocation densities. For controlled shock loading on well-characterized quartz powders, this broadening can be used as an indicator of peak shock pressure ("shock barometer"). Its use as a shock barometer for naturally shocked quartz has not yet been explored. To extrapolate this method to natural samples, more research is required to characterize the relaxation behavior of ^{29}Si in quartz and the influence of paramagnetic defects. The experimental conditions under which the NMR spectra are obtained (especially pulse recycle time) have a strong effect on the peak width. Therefore, to make use of ^{29}Si NMR spectral broadening as a quantitative measure of shock loading, it is imperative that these conditions be carefully controlled.

Broadening of the ^{29}Si NMR peak seems to be a general feature of shocked quartz, and we believe this technique may be more useful as a method for identifying naturally shocked quartz than for quantifying shock pressures. The primary contributor to the spectral broadening appears to be material with high shock-induced dislocation density. Preliminary data on the relaxation behavior of our samples indicate that the abundance of this extensively distorted material may be less than 1%, although the effect on the peak widths of the spectra obtained at a recycle time of 30 s is disproportionately large. Its T_1 relaxation time appears to be much shorter than that of the less distorted material, perhaps due to a higher concentration of paramagnetic centers associated with defects.

Unlike the results for quartz, the NMR spectra for the shocked An_{60} plagioclase feldspar have no features that obviously correlate with shock loading conditions. This result may be due to the already large peak breadth caused by the large number of silicon sites in its complex structure. There is no evidence to support the use of NMR spectroscopy of intermediate plagioclase as a shock barometer.

APPENDIX

Profile-fitting techniques are often used to accurately determine the characteristics of peaks associated with various spectroscopic methods. X-ray diffraction analysis often relies on an assortment of analytical functions for fitting to the observed diffraction pattern. *Howard and Snyder* (1983) and *Howard and Preston* (1989) provide details of the functions and discuss the benefits of each for the curve fitting of diffraction and other spectral peaks. These methods will usually provide a statistically accurate determination of peak position and intensity and a measure of the peak shape. The most commonly used fitting techniques are those that use Lorentzian and Gaussian functions. Equations (A1) and (A2) provide the analytical expressions used respectively for the Gaussian and Lorentzian curve fits to the observed spectral intensities

$$I = I_o \exp(-X^2/k) \quad (A1)$$

$$I = I_o (1 + k^2X^2)^{-1} \quad (A2)$$

X represents the deviation $(x_i - x_c)$ in the independent variable x_i from the peak center position x_c. I_o is the intensity of the peak at x_c. The k values are related to the peak width at half maximum (peak width) and are unique for each equation. In practice, the Lorentzian function is used to describe peaks that are characterized by broad tails, whereas the Gaussian function provides a description of narrow peaks. Lorentzian peaks provided the optimum peak shape for the deconvolution of our ^{29}Si NMR spectra into contributing components.

An additional function that combines the Lorentzian and Gaussian attributes for the empirical fitting of spectral data is the Pearson VII expression (*Brown and Edmonds*, 1980)

$$I = I_o [1 + 4/g^2 (2^{1/m} - 1) X^2]^{-m} \quad (A3)$$

The g term represents the full width of the peak at half maximum and the m exponent value refers to the curvature of the peak. Depending upon the value of m, this equation can provide an analytical function that is a linear combination of the Lorentzian and Gaussian expressions. The Pearson VII function (equation (A3)) reduces to the Lorenztian function (equation (A2)) when m is equal to unity. For practical purposes, the Pearson VII function approximates the Gaussian function (equation (A1)) when m has a value greater than 10.

The Pearson VII function is symmetrical about x_c and is limited in its ability to describe the observed X-ray patterns and NMR spectra for the quartz powders of this study. However, the asymmetry of the observed peaks can be evaluated by using a combination of two half-profiles of Pearson VII functions such that they share common I_o and x_c values. The so-called split Pearson VII function provides this flexibility. Figure A1 presents a schematic of the split Pearson VII curve for describing the spectral characteristics of a single broadened NMR peak. Six parameters are allowed to vary during the computerized least-squares fitting process in order to obtain the best fit of the split Pearson VII expression to the observed data. The peak width g will be the sum of the separate g_1 and g_2 values. This fitting technique was used here to derive the peak widths for the NMR and X-ray diffraction peaks.

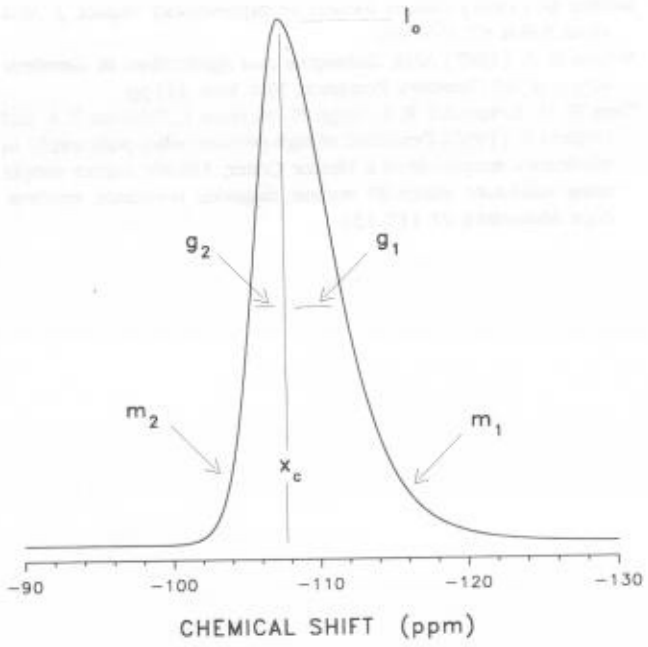

Fig. A1. Schematic of a split Pearson VII function applied to a broadened NMR peak. The resonance is described by six fitting parameters: maximum intensity I_o, peak center x_c, half peak widths g_1 and g_2 (peak width = $g_1 + g_2$), and curvature m_1 and m_2.

Acknowledgments. We would like to acknowledge the comments and careful reviews provided by two anonymous reviewers. We also thank C. Daniel, G. T. Holman, and M. Russell for their technical support and help during the shock recovery experiments. G. Turner contributed greatly to this work by his efforts in obtaining the MAS NMR spectra. Helpful scientific comments were provided by R. Assink, M. Carr, C. Hills, B. Morosin, B. Ristvet, and H. Westrich. This research was supported by the U.S. Department of Energy under contract DE-AC04-76DP00789 with partial funding from the Defense Nuclear Agency and National Science Foundation grant EAR90-04260 (R.J.K.).

REFERENCES

Alexopoulos J. S., Grieve R. A. F., and Robertson P. B. (1988) Microscopic lamellar deformation features in quartz: Discriminative characteristics of shock-generated varieties. *Geology, 16,* 796-799.

Bohor B. F., Foord E. E., Modreski P. J., and Triplehorn D. M. (1984) Mineralogic evidence for an impact event at the Cretaceous-Tertiary boundary. *Science, 224,* 867-869.

Brown A. and Edmonds J. W. (1980) The fitting of powder diffraction profiles to an analytical expression and the influence of line broadening factors. *Adv. X-ray Anal., 23,* 361-374.

Carter N. L. (1965) Basal quartz deformation lamellae—A criterion for recognition of impactites. *Am. J. Sci., 263,* 786-806.

Carter N. L., Officer C. B., Chesner C. A., and Rose W. I. (1986) Dynamic deformation of volcanic ejecta from the Toba caldera: Possible relevance to Cretaceous/Tertiary boundary phenomena. *Geology, 14,* 380-383.

Carter N. L., Officer C. B., Alexopoulos J. S., Grieve R. A. F., and Robertson P. B. (1989) Comment and reply on "Microscopic lamellar deformation features in quartz: Discriminative characteristics of shock-generated varieties." *Geology, 17,* 477-480.

Cygan R. T., Boslough M. B., and Kirkpatrick R. J. (1990) NMR spectroscopy of experimentally shocked quartz: Shock wave barometry. *Proc. Lunar Planet. Sci. Conf. 20th,* pp. 451-457.

De Carli P. S. and Milton D. J. (1965) Stishovite: Synthesis by shock wave. *Science, 147,* 144-145.

Deribas A. A., Dobretsov N. L., Kudinov V. M., and Zyuzin N. I. (1965) Shock compression of SiO_2 powders. *Dok. Akad. Nauk SSSR, 168,* 127-130.

Devreux F., Boilot J. P., Chaput F., and Sapoval B. (1990) NMR determination of the fractal dimension in silica aerogels. *Phys. Rev. Lett., 65,* 614-617.

Dupree E. and Pettifer R. F. (1984) Determination of Si-O-Si bond angle distribution in vitreous silica by magic angle spinning NMR. *Nature, 308,* 523-525.

French B. M. (1990) 25 years of the impact-volcanic controversy. *Eos Trans. AGU, 71,* 411-414.

French B. M. and Short N. M. (1968) *Shock Metamorphism of Natural Materials.* Mono, Baltimore. 644 pp.

Graham R. A. and Webb D. M. (1984) Fixtures for controlled explosive loading and preservation of powder samples. In *Shock Waves in Condensed Matter—1983* (J. R. Asay, R. A. Graham, and G. K. Straub, eds.), pp. 211-214. North Holland, New York.

Graham R. A. and Webb D. M. (1986) Shock-induced temperature distributions in powder compact recovery fixtures. In *Shock Waves in Condensed Matter—1985* (Y. M. Gupta, ed.), pp. 831-836. Plenum, New York.

Gratz A. J. (1984) Deformation in laboratory shocked quartz. *J. Non-Cryst. Solids, 67,* 543-558.

Gratz A. J., Tyburczy J., Christie J., Ahrens T., and Pongratz P. (1988) Shock metamorphism of deformed quartz. *Phys. Chem. Minerals, 16,* 221-233.

Grieve R. A. F. (1987) Terrestrial impact structures. *Annu. Rev. Earth Planet. Sci., 15,* 245-270.

Howard S. A. and Preston K. A. (1989) Profile fitting of powder diffraction patterns. In *Modern Powder Diffraction, Reviews in Mineralogy, Vol. 20* (D. L. Bish and J. E. Post, eds.), pp. 217-275. Mineralogical Society of America, Washington, DC.

Howard S. A. and Snyder R. L. (1983) An evaluation of some profile models and the optimization procedures used in profile fitting. *Adv. X-ray Anal., 26,* 73-81.

Kieffer S. W. (1971) Shock metamorphism of the Coconino Sandstone at Meteor Crater, Arizona. *J. Geophys. Res., 76,* 5449-5473.

Kirkpatrick R. J. (1988) MAS NMR spectroscopy of minerals and glasses. In *Spectroscopic Methods in Mineralogy and Geology, Reviews in Mineralogy, Vol. 18* (F. C. Hawthorne, ed.), pp. 341-403. Mineralogical Society of America, Washington, DC.

Kirkpatrick R. J., Smith K. A., Schramm S., Turner G., and Yang W. H. (1985) Solid-state nuclear magnetic resonance spectroscopy of minerals. *Annu. Rev. Earth Planet. Sci., 13,* 29-47.

Kirkpatrick R. J., Oestrike R., Weiss C. A., Smith K. A., and Oldfield E. (1986) High-resolution ^{27}Al and ^{29}Si NMR spectroscopy of glasses and crystals along the join $CaMgSi_2O_6$-$CaAl_2SiO_6$. *Am. Mineral., 71,* 705-711.

Kirkpatrick R. J., Carpenter M. A., Yang W. H., and Montez B. (1987) ^{29}Si magic-angle NMR spectroscopy of low-temperature ordered plagioclase feldspar. *Nature, 325,* 236-238.

Nicolaysen L. O. and Reimold W. U. (1990) *Cryptoexplosions and Catastrophes in the Geological Record, with a Special Focus on the Vredefort Structure.* Elsevier, Amsterdam. 422 pp.

Oestrike R., Yang W. H., Kirkpatrick R. J., Hervig R. L., Navrotsky A., and Montez B. (1987) High-resolution ^{23}Na, ^{27}Al, and ^{29}Si NMR spectroscopy of framework aluminosilicate glasses. *Geochim. Cosmochim. Acta, 51,* 2199-2209.

Pettifer R. F., Dupree R., Farnan I., and Sternberg U. (1988) NMR determinations of the Si-O-Si bond angle distributions in silica. *J. Non-Cryst. Solids, 106,* 408-412.

Ribbe P. (1983) *Feldspar Mineralogy, Reviews in Mineralogy, Vol. 2.* Mineralogical Society of America, Washington, DC. 362 pp.

Roddy D. J., Pepin R. O., and Merrill R. B. (1977) *Impact and Explosion Cratering.* Pergamon, New York. 1301 pp.

Smith J. V. and Blackwell C. S. (1983) Nuclear magnetic resonance of silica polymorphs. *Nature, 303,* 223-225.

Stöffler D. (1972) Deformation and transformation of rock-forming minerals by natural and experimental shock processes, I. Behavior of minerals under shock compression. *Fort. Mineral., 49,* 50-113.

Stöffler D. (1984) Glasses formed by hypervelocity impact. *J. Non-Cryst. Solids, 67,* 465-502.

Wilson M. A. (1987) *NMR Techniques and Applications in Geochemistry and Soil Chemistry.* Pergamon, New York. 353 pp.

Yang W. H., Kirkpatrick R. J., Vergo N., McHone J., Emilsson T. I., and Oldfield E. (1986) Detection of high-pressure silica polymorphs in whole-rock samples from a Meteor Crater, Arizona, impact sample using solid-state silicon-29 nuclear magnetic resonance spectroscopy. *Meteoritics, 21,* 117-124.